engineering proceedings

MDPI

Proceeding Paper

Optimization of Focused Ion Beam Patterning Parameters for Direct Integration of Plasmonic Nanostructures on Silicon Photodiodes †

E. Scattolo [1,2,*], A. Cian [1], D. Giubertoni [1], G. Paternoster [1], L. Petti [2] and P. Lugli [2]

[1] Sensors and Devices Center, Bruno Kessler Foundation, I-38123 Trento, Italy; email (A.C.); email (D.G.); email (G.P.)
[2] Libera Università Di Bolzano, Bozen, Italy; email (L.P.); email (P.L.)
* Correspondence: escattolo@fbk.eu
† Presented at the 8th International Electronic Conference on Sensors and Applications, 1–15 November 2021; Available online: https://ecsa-8.sciforum.net.

Abstract: The possibility to integrate plasmonic nanostructures directly on an active device, such as a silicon photodetector, is a challenging task of interest in many applications. Among the available nanofabrication techniques to realize plasmonic nanostructures, Focused Ion Beam (FIB) is surely the more promising, even if characterized by some limitations, such as ion implantation in the substrate. In this work, we demonstrate the direct integration of plasmonic nanostructures directly on an active Si-photodetector by patterning a silver film with FIB. To avoid ion implantation and therefore guarantee the unaltered device behavior, both the patterning parameters and the geometry of the nanostructures were implemented by Montecarlo and Finite-difference Time-domain simulations.

Keywords: silicon photodiode; plasmonic nanostructures; focused ion beam

Citation: Scattolo, E.; Cian, A.; Giubertoni, D.; Paternoster, G.; Petti, L.; Lugli, P. Optimization of Focused Ion Beam Patterning Parameters for Direct Integration of Plasmonic Nanostructures on Silicon Photodiodes. *Eng. Proc.* **2021**, *3*, x. https://doi.org/10.3390/xxxxx

Academic Editor: Elia Scattolo

Published: 1 November 2021

1. Introduction

In the last twenty years, many theoretical studies have shown that plasmonic structures have astonishing, unique, and interesting optical characteristics [1–4]. As a direct consequence, many scientific and industrial applications tried to take advantages of plasmonic s, leading also to substantial innovation in nanofabrication methods. As an example, the combination of plasmonic nanostructures with complementary metal-oxide-semiconductor (CMOS) optical sensors, capable of converting photons into electrical signals, raised a great interest, due to potentiality of extending the spectral responsivity of Silicon in a wider spectral region, from the ultra-violet (UV) up to the near infra-red (NIR) [5]. Unlike the fabrication of plasmonic nanostructures on an inert substrate, the production of plasmonic nanostructures on active sensors requires consideration of not only the surface topography but also the sensors' active behaviors. Therefore the choice of the production technique requires special considerations. Focused Ion Beam (FIB), which does not require a mask or a photoresist (as the ion beam is focused directly on the material of interest), is one of the methods for fabricating CMOS technology-compatible nanostructures [6–9]. Main advantage of direct nano-patterning by FIB is the total flexibility it gives in terms of shape and aspect ratio. Nevertheless, direct patterning can cause ions implantation in the substrate, causing flaws and modifying the electrical behavior of the sensors [10]. Thus, to fabricate plasmonic nanostructures directly on the top of a CMOS sensors is pivotal to tune the FIB process parameters, such as beam energy and current, dose and ions species. In this contribution, we demonstrate the integration of metallic plasmonic nanoarrays directly on top of an active silicon photodetector by FIB

patterning, showing no damage of the active behavior of the device. Both the structures and the patterning parameters were optimized by Finite-Difference Time-Domain (FTDT) and Montecarlo simulations, while the unaltered Si-detector behavior was evaluated by current-voltage (I–V) measurements.

Plasmonic Enhancement Optical Sensors

Among photon detecting systems, single photon avalanche diodes (SPADs) have been studied consistently during last years with the purpose to get higher detection efficiency and high timing resolution. Specifically, many applications are interested in having a high time resolution device to exploit near infrared (NIR), such as LiDAR (at 850–950 nm wavelengths), NIR spectroscopy, quantum computation, and detection of light from NIR emitting scintillators [11–14]. Differently from Silicon photodiodes (PDs), which have a thicker active region that can be employed to achieve higher efficiency in NIR region, SPADs need thinner active regions for technological and related to the time resolution required [15]. Hence, the integration of plasmonic metallic nanostructures supporting highly superficial confined light in a thin SPAD is a breakthrough solution to overcome this limitation. Recently, some interesting nanostructures have been investigating: (i) 1- and 2-dimensional gratings [16]; (ii) bullseye structures [17]; (iii) nano-pillars and nano-holes arrays [18]. Among those, in this work 1-D and 2-D metallic nanogratings are investigated considering their feasibility and possible integration with Si based photodetector and CMOS technologies.

2. Methods

The plasmonic nanoarrays are directly integrated on a Silicon based photodiode, i.e., a device able to transduce incident light (photons) in measurable currents (electrons). The proposed structure is composed of 3 parts (excluding the photodetector [19]): dielectric material, metallic grating, and passivation layer on top, Figure 1b. The dielectric material has two fundamental aims: (i) passivation the surface of the detector and, (ii) guarantee of the excitation of the surface plasmon polaritons (SPPs). Silicon nitride (Si_3N_4) and silicon oxide (SiO_2) are the perfect candidates as dielectric material because of their process compatibility with CMOS technology and for their chemical compatibility with Si-based device. The optimal thickness for the dielectric layer (which maximizes the enhancement) depends on the material selected and from theoretical simulations for both it is in the range of 5–20 nm. To fabricate the metal grating, a direct pattern by FIB can be employed after the evaporation of silver by physical vapor deposition (PVD), [20]. After the patterning, a passivation layer (usually PMMA) is spin coated on top of the grating, to guarantee performance stability and to avoid metal oxide formation.

The enhancement of the Si-photodetector efficiency coupled with metallic grating is achievable due to the confinement of photons (by the nanostructure) at the interface by the excitation of the SPPs, [21–23]. The wavelength at which the SPPs is excited and, therefore, the confinement of the photons is achieved, is function of grating geometry, dielectric thickness, and passivation thickness. Moreover, the direct integration of metallic plasmonic structures on top of an active device without damaging its behavior is a challenging task. Therefore, before starting the fabrication, both Montecarlo simulations [24,25] and FDTD [26] simulations were run, respectively to tune the ion beam parameters and to optimize the gratings geometry.

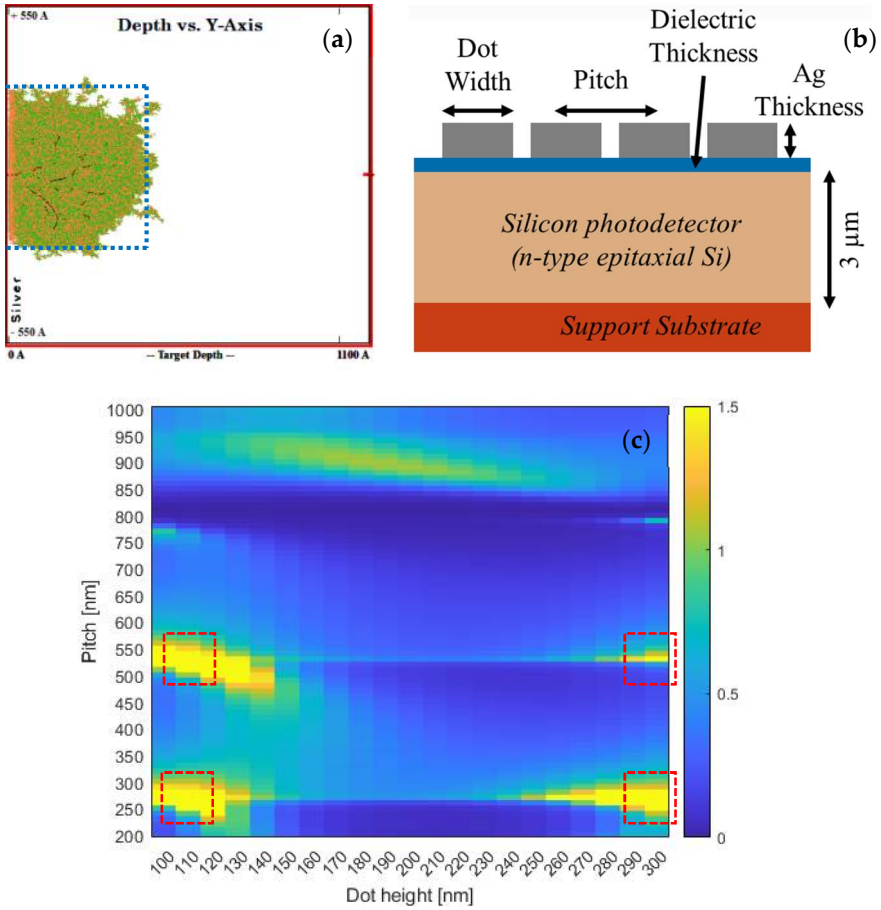

Figure 1. (**a**) Collision cascade from Montecarlo simulations inside silver layer; (**b**) Schematic cross section of the proposed device, from top: silver nanograting, silicon nitride dielectric, silicon photodetector; (**c**) Finite-difference time-domain [26] of simulated absorption at a wavelength of 950 nm normalized to the absorption of silicon covered with perfect anti reflective coating (PARC).

2.1. Montecarlo Simulations

As discussed before, the Montecarlo simulations are fundamental to tune the ion beam parameters. The aim of the simulations is to find the correct parameters to mill the silver layer without induces damages inside the active region of the device. The ion-solid interaction is theoretically simulated by a static interaction simulative software called SRIM concerning the **S**topping and **R**ange of **I**ons in **M**atter (SRIM), [24,25]. In Figure 1a, the theoretical collision cascade of gold double charged ions at 35 keV in silver layer is shown. The collision cascade exhibits a box shape (blue dotted line) close to the ideal configuration, with a sputter yield of 15.6 atoms per incident ion. The sputter yield is a fundamental parameters for FIB patterning because it indicates the number of sputtered atoms per each incident ion, hence, the higher it is, the higher is the number of removed atoms and therefore the faster is the patterning process. The sputter yield is also necessary to calculate the dose, i.e., the charge left on the sample by the ion beam per centimeters square, usually expressed by µC/cm^2. The dose depends not only on the target material and the ion beam specie, but also on the thickness of the material to be milled, [23]. To calculate the dose required the followed formula is used:

$$\phi = \frac{\rho\, z}{\Upsilon} \tag{1}$$

where ϕ [µC/cm^3] is the dose necessary to mill the thickness z [nm], Υ is the sputter yield [atoms/ions] and, p is the volumetric density of the target material in [atoms/cm^3].

2.2. Finite-Difference Time-Domain Simulations

A schematic cross section of the proposed structures is shown in Figure 1b, the silver nanoarrays was selected because they allow exploiting hybrid opto-plasmonic resonances in the NIR as result of the spectral matching between the surface plasmons polaritons at a metal-dielectric interface and the Rayleigh anomaly [27].

Therefore, the optimization of the geometrical parameters of the nanoarrays to enhance absorption in the NIR range inside the photodetector are run by FDTD simulations [26]. In Figure 1c, an overview of the simulations run to the optimization of the nanoarrays structure is shown. The aim of the simulations in the Figure 1c is to determine the best values of metal thickness (dot height, x-axis) and periodicity (pitch, y-axis) to have the highest quantum efficiency (QE) at 950 nm, i.e., the highest number of collected electrons over the number of incident ions.

The QE shows in Figure 1c is normalized respect the maximum value of QE obtained by coupling the same Si-photodetector to a perfect anti reflective coating (PARC) i.e., a stack of different material layers with tuned refractive index able to almost null the fraction of reflected light incident on the device. The simulations highlight 4 couples of metal thickness and pitch values:

The values reported in Table 1 are referred for both 1-dimensional (1D) and 2-dimensional (2D) arrays, with the following nomenclature "p-xyz,h-abc", where p stands for pitch and xyz is the values of the pitch in nm, and where h stands for height and abc is the values of the metal thickness in nm. The fabrication of silver nanoarrays with the specific values reported in Table 1 presents some challenging features. The nanoarrays with p-535, h-110 are the most replicable in both the configurations 1D and 2D. By contrary, the p-535, h-300 cannot be fabricated by FIB patterning but the long dwell time (time spent by the ion beam on each point to mill the material) necessary to mill 300 nm thickness of silver would lead to a (i) low lateral definition of the structures and, to an (ii) too long patterning time. Hence, the configuration p-535, h-300 is not considered and for the same reasons also the configuration p-260, h-300. Similar is the fabrication of p-260, h-110 which presents some tricky features because of the high aspect ratio and the low beam spot size required. For the above cited reasons, only the configuration with the lower metal thickness (p-535,h-110 and p-260,h-110) both 1-D and 2-D are considered in this work. To characterize the electrical behavior of the enhanced detector, the device was electrically connected by gold wire bonding to a printed circuit board (PCB) which presents 24 pins: 20 for photodiode metal contact and 4 for reference.

Table 1. Reported couples of metal thickness and periodicity values at absorption peaks from Figure 1c.

	p-535, h-110	**p-535, h-300**	**p-260, h-110**	**p-260, h-300**
Metal thickness [nm]	110	300	100	300
Periodicity [nm]	535	535	260	260

3. Results and Discussion

In the previous section, the results of the Montecarlo and FDTD simulations are reported and discussed. Hence, both the patterning parameters and geometry features are optimized to guarantee a working integrated Si-detector with a higher efficiency in the NIR region. The two configurations p-535,h-100—p-260,h-110 in both 1-D and 2-D geometry were nanofabricated by FIB technique with gold doubled charge ions with an energy of 35 keV, a beam current of 19 pA and, a dose value calculated by Equation (1). The SEM images of the patterned nanostructures are shown in Figure 2, the 1-D and 2-D nanoarrays at higher periodicity (p-535) and the 1-D nanoarray at smaller periodicity (p-260) present a better reproducibility and conformity, on the other hand, the 2-D nanoarrays at smaller pitch (p-260) shows a very low conformity in the shape and dimension of the dots, probably as results of relatively too big spot beam.

As discussed before, the main limitation of direct patterning of nanostructures directly on active device by FIB is the possible damaging of the device for ion implantation. Moreover, using gold ions as beam specie is a challenging choice because gold has been always considering "Silicon-killer" since the early development of the silicon-based technology, ref. [28] therefore, just a low concentration of gold ions inside the device could completely make the device useless. The evaluation of the unaltered state of the device was assessed by dark current measurements, which is the current flowing inside the device under the condition of no illumination. In a working silicon detector, the dark current, also called noise, should be at least 3 orders of magnitude less than the generated currents under illumination. The current generated under illumination has on average an intensity of hundreds of μA in the silicon photodetector produced in the Fondazione Bruno Kessler's facilities. In Table 2 the values of dark current measured at reverse applied voltage of 2 V of the four configurations show in Figure 2 are reported. All four the values of noise reported are in the order of tens of pA and comparable with the noise value of the reference diode (a not nanostructured diode). The dark currents reported in Table 2 are at least 5 order of magnitude lower than the current generated under illumination (hundreds of μA). Therefore, the gold-ion patterning of silver directly on Si-photodiode does not damage the active behavior of the device, and the integration is successful.

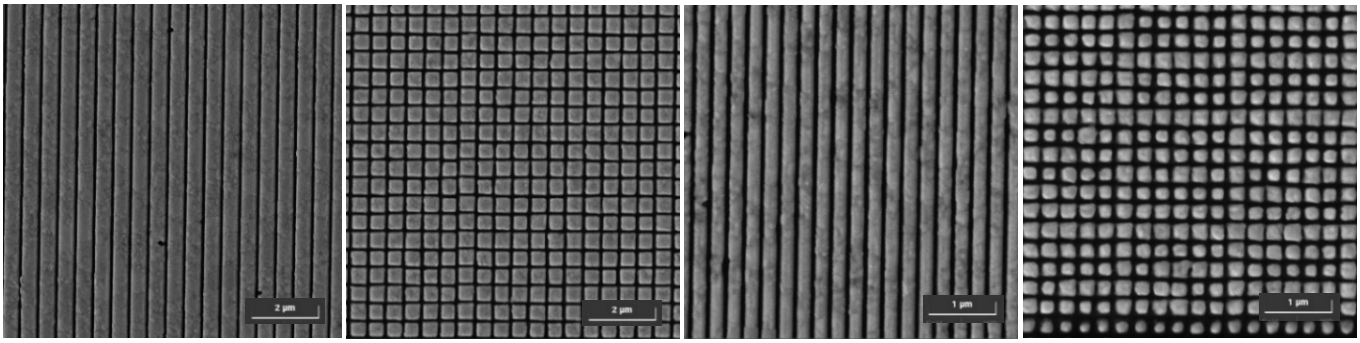

(**a**) (**b**) (**c**) (**d**)

Figure 2. SEM images of the configuration (**a**) 1D p-535, (**b**) 2D p-535, (**c**) 1D p-260 and, (**d**) 2D p-260.

Table 2. Reported values of dark current of reference diodes (naked) and photodiodes patterned by FIB at 2V in reverse mode.

Reference	FIB 1D	FIB 2D
	p-535, h-110	**p-535, h-110**
21 pA	41 pA	25 pA
	p-260, h-110	**p-260, h-110**
	10 pA	37 pA

4. Conclusions

The ability to integrate plasmonic nanostructures directly on silicon photodiodes is of interest in many scientific and industrial, mainly because of the unique optical properties plasmonic structures can offer. Nevertheless, the characteristic size and the geometry of the plasmonic structures are typically not of easy fabrication. In this work, we demonstrated that FIB technique is a solid solution to nanopattern the plasmonic structures directly on an active device by the optimization of the patterning parameters and geometrical parameters by Montecarlo and FDTD simulations, respectively. In this contribution, we report the successful integration of metallic plasmonic structures on silicon photodiode without inducing any irreversible damage in the active region of the device. Results are demonstrated by the unaltered value of the dark current of the

patterned diodes. This paves the way to further applications given by the integration of plasmonic nanostructures with photodetectors, such as plasmonic biosensors all-in-one.

Author Contributions: Conceptualization, G.P. and E.S.; methodology, E.S., G.P. and D.G.; software, E.S. and D.G.; validation, E.S., D.G. and G.P.; formal analysis, E.S. and A.C.; investigation, E.S., A.C. and D.G.; writing—original draft preparation, E.S.; writing—review and editing, L.P. and G.P.; visualization, A.C. and D.G.; supervision, G.P., D.G., L.P. and P.L.; project administration, G.P. and D.G.; funding acquisition, G.P. and D.G. All authors have read and agreed to the published version of the manuscript.

Funding: This project has received funding from the EU-H2020 research and innovation programme under Grant Agreement 777222 ATTRACT project "PlaSiPM" and under grant agreement No 654360 NFFA-Europe.

Institutional Review Board Statement:

Informed Consent Statement:

Data Availability Statement:

Conflicts of Interest: The authors declare no conflict of interest.

References

1. Konstantatos, G.; Sargent, E.H. Nanostructured materials for photon detection. *Nat. Nanotechnol.* **2010**, *5*, 391–400, doi:10.1038/nnano.2010.78.
2. Soci, C.; Zhang, A.; Bao, X.Y.; Kim, H.; Lo, Y.; Wang, D. Nanowire photodetectors. *J. Nanosci. Nanotechnol.* **2010**, *10*, 1430–1449.
3. Schuller, J.A.; Barnard, E.; Cai, W.; Jun, Y.C.; White, J.S.; Brongersma, M.L. Plasmonics for extreme light concentration and manipulation. *Nat. Mater.* **2010**, *9*, 193–204, doi:10.1038/nmat2630.
4. Ghosh, B.; Espinoza-Gonzales, R. Plasmonics for Improved Photovoltaic Devices. *Online J. Mater. Sci.* **2017**.
5. Gola, A.; Acerbi, F.; Capasso, M.; Marcante, M.; Mazzi, A.; Paternoster, G.; Piemonte, C.; Regazzoni, V.; Zorzi, N. NUV-Sensitive Silicon Photomultiplier Technologies Developed at Fondazione Bruno Kessler. *Sensors* **2019**, *19*, 308, doi:10.3390/s19020308.
6. Kim, C.-S.; Ahn, S.-H.; Jang, D.-Y. Review: Developments in micro/nanoscale fabrication by focused ion beams. *Vacuum* **2012**, *86*, 1014–1035, doi:10.1016/j.vacuum.2011.11.004.
7. Wilhelmi, O.; Reyntjens, S.; Mitterbauer, C.; Roussel, L.; Stokes, D.J.; Hubert, D.H.W. Rapid Prototyping of Nanostructured Materials with a Focused Ion Beam. *Jpn. J. Appl. Phys.* **2008**, *47*, 5010–5014, doi:10.1143/jjap.47.5010.
8. Rubanov, S.; Munroe, P. The application of FIB milling for specimen preparation from crystalline germanium. *Micron* **2004**, *35*, 549–556, doi:10.1016/j.micron.2004.03.004.
9. Schoendorfer, C.; Lugstein, A.; Bischoff, L.; Hyun, Y.; Pongratz, P.; Bertagnolli, E. FIB induced growth of antimony nanowires. *Microelectron. Eng.* **2007**, *84*, 1440–1442, doi:10.1016/j.mee.2007.01.070.
10. Xu, X.; Wu, J.; Wang, X.; Zhang, M.; Li, J.; Shi, Z.; Li, H.; Zhou, Z.; Ji, H.; Niu, X.; et al. Ion-Beam-Directed Self-Ordering of Ga Nanodroplets on GaAs Surfaces. *Nanoscale Res. Lett.* **2016**, *11*, 38, doi:10.1186/s11671-016-1234-y.
11. Kawano, Y.; Fuse, T.; Toyokawa, S.; Uchida, T.; Ishibashi, K. Terahertz photon-assisted tunneling in carbon nanotube quantum dots. *J. Appl. Phys.* **2008**, *103*, 034307, doi:10.1063/1.2838237.
12. Komiyama, S. Single-Photon Detectors in the Terahertz Range. *IEEE J. Sel. Top. Quantum Electron.* **2011**, *17*, 54–66, doi:10.1109/jstqe.2010.2048893.
13. Pan, Z.W.; Dai, Z.R.; Wang, Z.L. Nanobelts of Semiconducting Oxides. *Angew. Chem. Int. Ed. Engl.* **1996**, *118*.
14. Iijima, S. Helical microtubules of graphitic carbon. *Nature* **1991**, *354*, 56–58, doi:10.1038/354056a0.
15. Takai, I.; Matsubara, H.; Soga, M.; Ohta, M.; Ogawa, M.; Yamashita, T. Single-Photon Avalanche Diode with Enhanced NIR-Sensitivity for Automotive LIDAR Systems. *Sensors* **2016**, *16*, 459, doi:10.3390/s16040459.
16. Niu, C.; Huang, T.; Hu, J. Plasmonic Nanograting Structures for Sensor Applications, Texas Symposium on Wireless and Microwave Circuits and Systems. In Proceedings of the Texas Symposium on Wireless and Microwave Circuits and Systems, Waco, TX, USA, 3–4 April 2014.
17. Andersen, S.K.H.; Bogdanov, S.; Makarova, O.; Xuan, Y.; Shalaginov, M.Y.; Boltasseva, A.; Bozhevolnyi, S.I.; Shalaev, V.M. Hybrid Plasmonic Bullseye Antennas for Efficient Photon Collection. *ACS Photon* **2018**, *5*, 692–698, doi:10.1021/acsphotonics.7b01194.
18. Caldwell, J.D.; Glembocki, O.; Bezares, F.J.; Bassim, N.D.; Rendell, R.W.; Feygelson, M.; Ukaegbu, M.; Kasica, R.; Shirey, L.; Hosten, C. Plasmonic Nanopillar Arrays for Large-Area, High-Enhancement Surface-Enhanced Raman Scattering Sensors. *ACS Nano* **2011**, *5*, 4046–4055, doi:10.1021/nn200636t.
19. Gola, A.; Acerbi, F.; Capasso, M.; Marcante, M.; Mazzi, A.; Paternoster, G.; Piemonte, C.; Regazzoni, V.; Zorzi, N. NUV-Sensitive Silicon Photomultiplier Technologies Developed at Fondazione Bruno Kessler. *Sensors* **2019**, *19*, 308, doi:10.3390/s19020308.
20. Selvakumar, N.; Barshilia, H. Review of physical vapor deposited (PVD) spectrally selective coatings for mid- and high-temperature solar thermal applications. *Sol. Energy Mater. Sol. Cells* **2012**, *98*, 1–23, doi:10.1016/j.solmat.2011.10.028.

21. Stanley Middleman, B.; Hochberg, A.K. *Process Engineering Analysis in Semiconductor Device Fabrication*; Mcgraw-Hill College: New York, NY, USA, 1993.
22. Newman, T.H. High resolution patterning system with a single bore objective lens. *J. Vac. Sci. Technol. B: Microelectron. Nanometer Struct.* **1987**, *5*, 88, doi:10.1116/1.583934.
23. Orloff, J.; Utlaut, M.; Swanson, L. High Resolution Focused Ion Beams: FIB and its Applications. In *High Resolution Focused Ion Beams: FIB and Its Applications*; Springer Science and Business Media LLC: Berlin/Heidelberg, Germany, 2003.
24. Ziegler, J.F.; Biersack, J.P.; Ziegler, J.F. Watson, The stopping and range of ions in matter. 1960.
25. Ziegler, J.F.; Ziegler, M.D.; Biersack, J.P. SRIM—The stopping and range of ions in matter (2010). *Nucl. Instrum. Methods Phys. Res. Sect. B Beam Interact. Mater. Atoms* **2010**, *268*, 1818–1823.
26. Lumerical: High-Performance Photonic Simulation Software. Available online: www.lumerical.com (accessed on 22 September 2021).
27. A Maradudin, A.; Simonsen, I.; Polanco, J.; Fitzgerald, R.M. Rayleigh and Wood anomalies in the diffraction of light from a perfectly conducting reflection grating. *J. Opt.* **2016**, *18*, 024004, doi:10.1088/2040-8978/18/2/024004.
28. Davis, G.L. Gold in semiconductor technology. *Gold Bull.* **1974**, *7*, 90–96, doi:10.1007/bf03215044.